PROCEEDINGS OF SPIE

SPIEDigitalLibrary.org/conference-proceedings-of-spie

A review of the growth, doping, and applications of β-Ga₂ beta;-Ga₂

Manijeh Razeghi, Ji-Hyeon Park, Ryan McClintock, Dimitris Pavlidis, Ferechteh H. Teherani, et al.

Manijeh Razeghi, Ji-Hyeon Park, Ryan McClintock, Dimitris Pavlidis, Ferechteh H. Teherani, David J. Rogers, Brenden A. Magill, Giti A. Khodaparast, Yaobin Xu, Jinsong Wu, Vinayak P. Dravid, "A review of the growth, doping, and applications of β-Ga₂O₃thin films," Proc. SPIE 10533, Oxide-based Materials and Devices IX, 105330R (14 March 2018); doi: 10.1117/12.2302471



Event: SPIE OPTO, 2018, San Francisco, California, United States

A Review of the Growth, Doping & Applications of β-Ga₂O₃ thin films

Manijeh Razeghi^{1*}, Ji-Hyeon Park¹, Ryan McClintock¹, Dimitris Pavlidis², Ferechteh H. Teherani³, David J. Rogers³, Brenden A. Magill⁴, Giti A. Khodaparast⁴, Yaobin Xu^{5,6}, Jinsong Wu^{5,6}, Vinayak P. Dravid^{5,6}

¹Center for Quantum Devices, Department of Electrical Engineering and Computer Science, Northwestern University, Evanston, Illinois 60208, USA; ²College of Engineering, Department of Electrical and Computer Engineering, Boston University, Boston, Massachusetts, United States; ³Nanovation, 8 route de Chevreuse, 78117 Chateaufort, France; ⁴Department of Physics, Virginia Tech, Blacksburg, VA, 24061, USA; ⁵ Department of Materials Science and Engineering, Northwestern University, Evanston, IL 60208, USA; ⁶ NUANCE Center, Northwestern University, Evanston, IL 60208, USA

ABSTRACT

 β -Ga₂O₃ is emerging as an interesting wide band gap semiconductor for solar blind photo detectors (SBPD) and high power field effect transistors (FET) because of its' outstanding material properties including an extremely wide bandgap (Eg ~4.9eV) and a high breakdown field (8 MV/cm). This review summarizes recent trends and progress in the growth/doping of β -Ga₂O₃ thin films and then offers an overview of the state-of-the-art in SBPD and FET devices. The present challenges for β -Ga₂O₃ devices to penetrate the market in real-world applications are also considered, along with paths for future work.

Keywords: Ga₂O₃, Solar blind photo detectors, Thin films

1. INTRODUCTION

Ultra-wide bandgap (UWBG) semiconductors represent a highly exclusive club which comprises very diverse materials including AlN, BN, and diamond. It is only recently that Ga_2O_3 has been considered a full member of the club based on a number of breakthroughs including the development of commercial single crystal substrates and the demonstration of n-type doping with reasonably high mobilities. Table 1 shows the space group, structure and lattice constant summaries for Ga_2O_3 . It can be seen from the table that Ga_2O_3 has five different polymorphs (α -, β -, γ -, δ - κ - and ϵ), amongst which monoclinic β - Ga_2O_3 is thermodynamically the most stable 1 . Thus, the majority of the application studies on Ga_2O_3 have been focused on β - Ga_2O_3 .

Polymorph	α^2	β^3	γ^4	$\mathbf{\epsilon}^{5}$	κ^6
Space group	R-3c	C2/m	Fd-3m	P6 ₃ mc	$Pna2_1$
Structure	rhombohedral	monoclinic	cubic	hexagonal	orthorhombic
Lattice parameter	a=4.9825Å c=13.433Å	a=12.214 (3)Å b=3.0371(9)Å c=5.7981(9)Å β=103.83(2)°	$a=8.238 \rm{\mathring{A}}$	a = 2.9081(7)Å c = 9.262(3)Å	a = 5.0557(1) Å b = 8.68842(9) Å c = 9.27585(6) Å

Table 1. Summary of Ga₂O₃ polymorphs. (δ-Ga₂O₃ is a nanocrystalline form of ε-Ga₂O₃ and not a distinct polymorph.)⁶

Oxide-based Materials and Devices IX, edited by David J. Rogers, David C. Look, Ferechteh H. Teherani, Proc. of SPIE Vol. 10533, 105330R ⋅ © 2018 SPIE CCC code: 0277-786X/18/\$18 ⋅ doi: 10.1117/12.2302471

^{*}Invited corresponding author: razeghi@eecs.northwestern.edu

 β -Ga₂O₃ is a very interesting material system combining an UWBG (~ 4.9 eV) with a decent mobility (~100 cm²/Vs), a high breakdown field (8 MV/cm) and good thermal/chemical stability. It is thus being considered as a new alternative to SiC and GaN for use in high power electronics⁷⁻¹² and ultra violet (UV)C solar blind photodetectors (SBPD). β -Ga₂O₃ thin film n-type carrier concentration can be tuned the from low 10¹⁷ cm⁻³ up to 10¹⁹ cm⁻³ by doping with, for instance, Si, Ge or Sn. ¹³⁻¹⁵ Furthermore, similar to GaN, β -Ga₂O₃ has shown the potential to form a two-dimensional electron gas (2DEG) at (Al_xGa_{1-x})₂O₃/Ga₂O₃ hetero-interfaces and thus offers a basis for the development of high electron mobility transistors (HEMTs).

A key drawback of β-Ga₂O₃ till present has been lack of a reliable method for fabricating p-type β -Ga₂O₃²⁹. Up till now, therefore, β-Ga₂O₃ power device studies have been mainly based on homoepitaxial isotype devices grown on semi-insulating substrates. Various architectures have been demonstrated, including metal-semiconductor field-effect transistors (MESFETs), metal-oxide-semi- conductor field-effect transistors (MOSFETs), and fin-array field-effect transistors (FinFETs) ^{7,8,16-18}. High quality heteroepitaxial β-Ga₂O₃ thin films have also been grown using non-native substrates such as a-, r-, c-sapphire, silicon, MgO and yttrium-stabilized zirconia (YSZ)¹⁹⁻²¹. Many growth techniques have been adopted, such as molecular beam epitaxy (MBE), atomic layer deposition (ALD), halide vapor phase epitaxy (HVPE) and metal organic chemical vapor deposition (MOCVD) ²¹⁻²⁸. However, when β-Ga₂O₃ thin films are grown on non-native substrates, it has proven challenging to control n-type doping concentration due to the occurrence of defects, such as stacking faults and threading dislocations caused by the lattice and thermal expansion mismatches between the non-native substrate and β-Ga₂O₃ thin films.

In this paper, we briefly review the growth, doping and applications of β -Ga₂O₃ thin films.

2. GROWTH OF BETA-GALLIUM OXIDE THIN FILMS

In order for β -Ga₂O₃ to be used in electronic and optoelectronic devices, thin film growth technology should be given priority. In this section we overview the state-of-the-art of β -Ga₂O₃ thin film growth by CVD, MOCVD, MBE and ALD^{19,30-32}.

2.1 Growth of β-Ga₂O₃ thin films by CVD

The CVD process is a simple and efficient method for growing a thin film by supplying vapor precursors to the substrate. Pure Ga pellets tend to be used as a Ga source rather than gallium trichloride $GaCl_3$ or $GaCl_{19,33-36}$. A comparative study of c-plane (0001), a-plane (11-20), and r-plane (1-102) sapphire substrates for the low pressure chemical vapor deposition (LPCVD) of β -Ga₂O₃ thin films was conducted by Rafique et al ¹⁹. High purity gallium pellets (Alfa Aesar, 99.99999%) and oxygen were used as precursors. The growth on c-plane sapphire gave the purest monoclinic β -Ga₂O₃ thin films with a (-201) orientation while the a-plane sapphire yielded a β -Ga₂O₃ phase exhibiting a dominant (111) orientation. In the thin film growth on r-plane sapphire, α -phase mixed with β -phase was obtained. The corresponding field emission scanning electron microscopy (FE-SEM) images are shown in Figure 1.

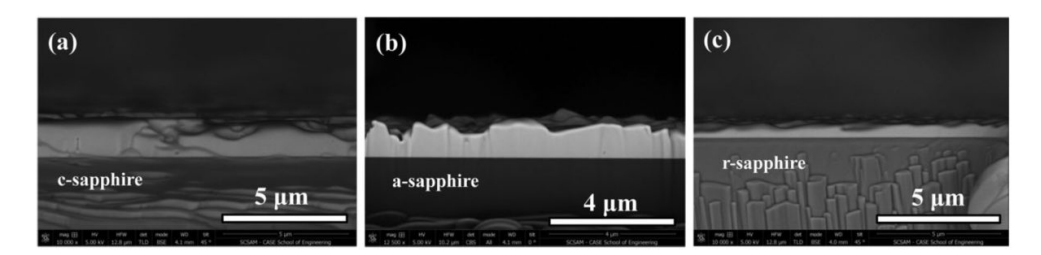


Figure 1. Cross-sectional FESEM images of the Ga₂O₃ thin films grown on differently oriented sapphire substrates: (a) c-plane sapphire, (b) a-plane sapphire, and (c) r-plane sapphire. [Reprinted with permission from ¹⁹ Copyright (2016) John Wiley and Sons.]

The Ga_2O_3 thin films were grown on the c-, a- and r-plane sapphire substrates at 900 °C. The growth rates were estimated as 1.1 µm/h, 1.8 µm/h, and 0.4 µm/h, respectively. Terasako et al. reported on β - Ga_2O_3 thin films and nanostructures grown on c-sapphire substrate by atmospheric-pressure CVD (AP-CVD) using metal Ga (Nacalai Tesque, Purity 99.9999%) beads and H_2O as precursors 34 . Molecular N_2 was used as a gas and, when the growth temperature was 850°C, highly (-201) oriented polycrystalline β - Ga_2O_3 films having a relatively flat surface were obtained. Kaneko et al. proposed fabrication of (-201) oriented β - Ga_2O_3 thin films on YSZ substrates using a Mist CVD technique 32 . In Mist-CVD liquid solution precursors are atomized with an ultrasonic transducer to generate a mist with which to grow thin films. Comparatively flat β - Ga_2O_3 thin films containing polycrystal precipitates were achieved on YSZ (100) substrates for a growth temperature of 650 °C. Figures 2 (a) and (b) show an electron diffraction pattern of crystal precipitates grown on the YSZ (100) substrate and a cross-sectional transmission electron microscopy (TEM) image of crystal precipitates composed of many crystal domains.

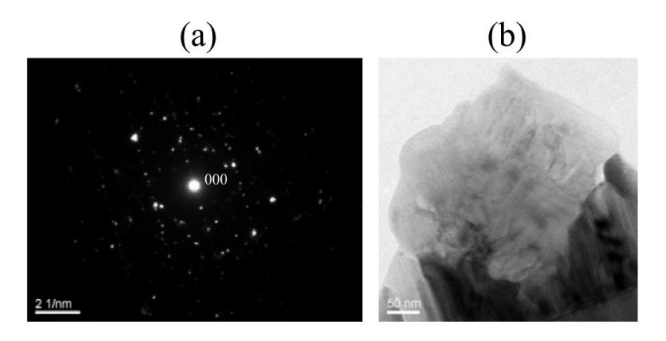


Figure 2. (a) Selected area electron diffraction (SAED) pattern for for large-scale precipitates in β-Ga₂O₃ thin films grown on YSZ (100) substrates and (b) a cross-sectional TEM images of a typical such precipitate. [Reprinted with permission from 32 Copyright (2013) John Wiley and Sons.]

2.2 Growth of Ga₂O₃ thin films by MOCVD

MOCVD is well established for its' potential to cost-effectively grow high-quality epitaxial thin films on an industrial scale at relatively high growth rates. In MOCVD, β -Ga₂O₃ thin films are usually grown using Ga precursors such as trimethylgallium (TMGa) and triethylgallium (TEGa). High purity O₂, N₂O, and high pure water are generally used as oxygen precursors. To control the carrier concentration, precursors such as tetraethylorthosilicate (TEOS), tetraethyltin (TESn) and bis(cyclopentadienyl)magnesium (Cp₂Mg) are typically used for Si, Sn and Mg, respectively. N₂, Ar and H₂ are commonly adopted as carrier gases to deliver the MO (metalorganic) source to the reactor. ^{13,15,27,28,37–43}. Various experiments using non-native substrates have been carried out to explore the potential of heteroepitaxy for β-Ga₂O₃ thin films ^{15,26,44}. Feng et al. reported growth of Mg doped β-Ga₂O₃ thin films on c-sapphire substrates using MOCVD. Amorphous or nanocrystalline Mg-doped Ga₂O₃ was transformed into a polycrystalline monoclinic structure (0-3 at%)Mg-doped β-Ga₂O₃ with (-201) orientation by annealing at 800 °C for 60 minutes ³⁹.

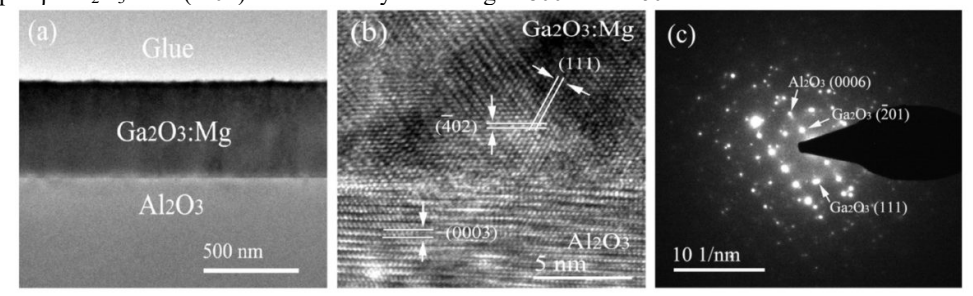


Figure 3. (a) Low magnification TEM, (b) HRTEM and (c) SAED micrographs of the interface between the annealed 3% Mg-doped Ga_2O_3 film and α -Al₂O₃ substrate. [Reprinted with permission from ³⁹ Copyright (2016) Elsevier.]

Figure 3 (a), (b) and (c) are a low magnification cross-sectional TEM image, an HR-TEM image, and a SAED pattern of the interface between the annealed 3 % Mg-doped Ga_2O_3 film and the $Al_2O_3(0001)$ substrate, respectively. As can be seen from the SAED pattern, diffraction spots and some dispersive diffraction rings are observed due to the presence of epitaxial and polycrystalline components in the film. Highly (-201) oriented crystal β- Ga_2O_3 thin films were grown on c-sapphire substrates at 450 °C by Ravadgar et al. It was found that when the films were subsequently annealed in air at 700 and 800 °C for 30 minutes their surface states and point defects were partially healed 40 . Gogova et al. compared β- Ga_2O_3 thin films grown by low-pressure MOCVD using c-sapphire and β- Ga_2O_3 (100) substrates 15,26 . Tadjer et al. studied epitaxial growth of monoclinic β- Ga_2O_3 thin films on a- and c-plane sapphire by MOCVD. Smooth surface morphology was obtained on c-sapphire, and the films were highly (-201) oriented 44 . Recently, studies reported on the formation of β- Ga_2O_3 thin films, through transformation from other phases (α -, β -, γ -, δ - κ - and ϵ) $^{45-47}$. Study of ϵ -phase polymorph thin films by MOCVD has been reported by Fornari et al 48 . In this experiment, ϵ - Ga_2O_3 thin films were grown on c-sapphire with TMGa and ultrapure water as precursors of Ga and oxygen, respectively. Figure 4 shows the results of differential scanning calorimetry (DSC) measurements.

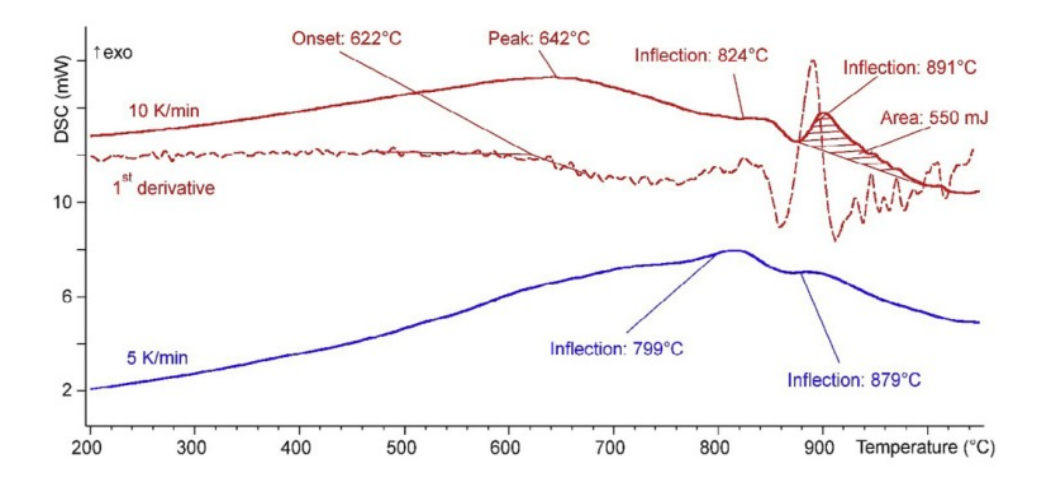


Figure 4. DSC curves of two ε-Ga₂O₃ layers on sapphire recorded at 10 and 5 K/min. The first derivative (DDSC) of the 10 K/min is also shown as a dashed line. [Reprinted with permission from ⁴⁸ Copyright (2017) Elsevier.]

Although some indication of lattice modifications are detected above about 650°C the ε-phase was able to withstand extended heat treatment up to 700°C and complete transition to β-Ga₂O₃ was only observed for temperatures ≥ 900°C. κphase polymorph thin films grown using MOCVD were also investigated⁴⁵. We (the authors of this review) have also grown κ-phase polymorph thin films at relatively low temperature of 690°C by MOCVD. TMGa and high purity deionized water (18 M Ω) were used as gallium and oxygen precursors, respectively. H₂ was used as the carrier gas. Figure 5 (a) is a cross-sectional bright-field TEM image showing the typical morphology of Ga₂O₃/ Al₂O₃ (001) film system. The film has a uniform thickness of about ~1.28 µm. The surface of the Ga₂O₃ film is quite flat without any terraces and fluctuations. It is noted that the film exhibits a high-density of line-like contrast threading through the whole film, but no obvious defects can be observed along the interface. SAED patterns as shown in Figure 5 (b) and (c) were taken along different zone axes in order to study the structure of the Ga₂O₃ film. Based on the SAED patterns, the κ phase (an analogue of orthorhombic κ-Al₂O₃ with the space group of Pna^2 1) was identified. Simulated SAED patterns (as shown in Figure 5 (d)) match well to the experimental ones. The presence of a certain type of ordering (and thus superstructure) is also deduced from the extra electron diffraction spots indicated by yellow arrows in Figure 5 (d). No other spots are observed, which is coherent with an absence of a secondary phase in the layer or a chemical reaction occurring at the film/substrate interface. Thus, by MOCVD, we have successfully synthesized stable κ-Ga₂O₃, (which is considered a transient phase in Ga₂O₃ ⁶).

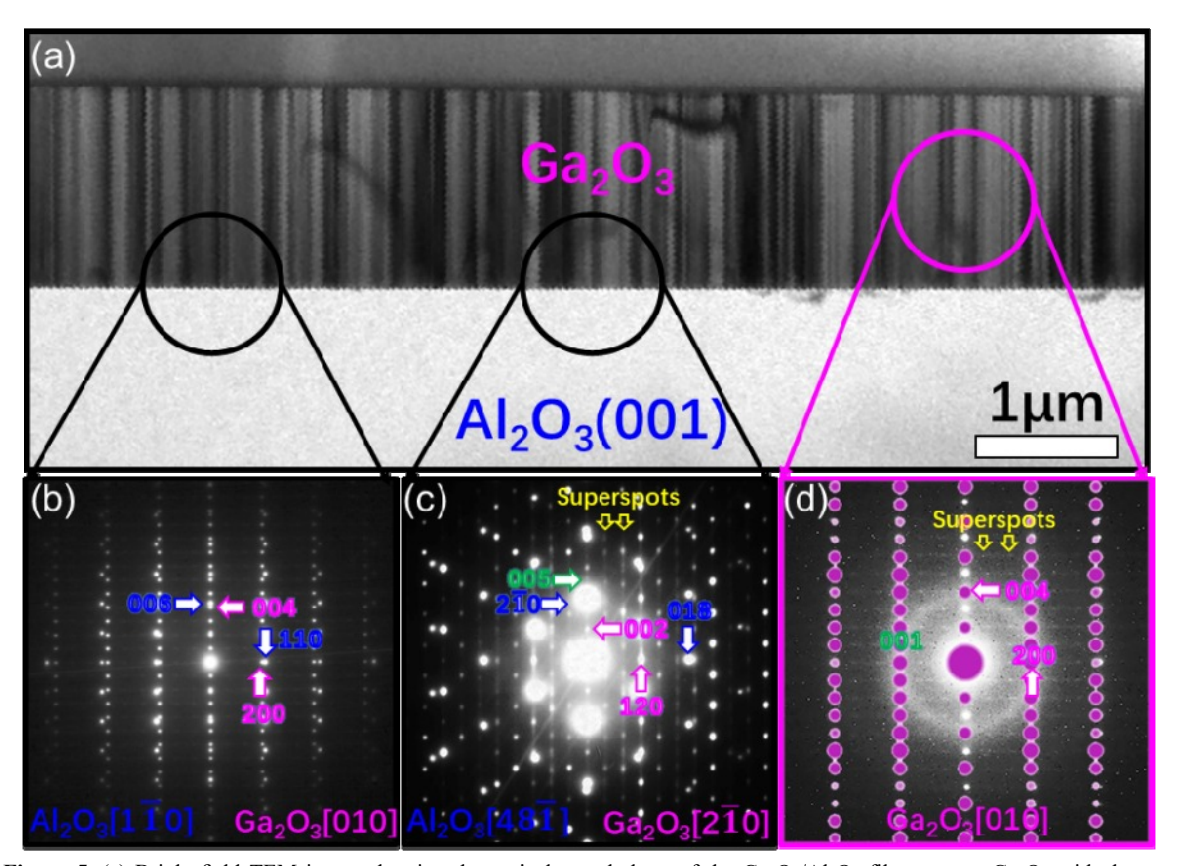


Figure 5. (a) Bright-field TEM image showing the typical morphology of the Ga₂O₃/Al₂O₃ film system. Ga₂O₃ with the space group *Pna*²1 is identified. Yellow arrows indicated extra diffraction spots are related to a high density of planar defects. Composite SAED patterns obtained (b) along the [010] zone axis at the Ga₂O₃/Al₂O₃ interface (c) along the [2-10] zone axis at the Ga₂O₃/Al₂O₃ interface (d) along the [010] zone axis for the Ga₂O₃ film. Simulated electron diffraction pattern imposed in (d) as purple spots is consistent with the experimental one (d).

Sbrockey et al. demonstrated the growth of β -Ga₂O₃ thin films on a 50-mm single-side-polished c-sapphire wafer and a 200-mm (100) silicon wafer ²⁸. TMGa and oxygen were used as precursors and Ar gas was used as a carrier gas. The growth behaviors of β -Ga₂O₃ thin films were investigated as a function of growth temperature, pressure and III/VI ratio.

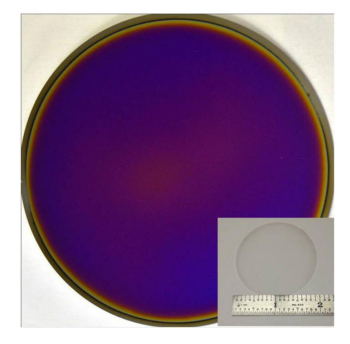


Figure 6. Photograph of a 200-mm (100) silicon wafer with MOCVD-deposited Ga₂O₃ film of nominal 90 nm thickness. The insert shows an MOCVD-deposited Ga₂O₃ film of nominal 320 nm thickness, on a 50-mm single-side-polished (0001) sapphire wafer. The size scale in the insert is applicable for both images. [Reprinted with permission from ²⁸ Copyright (2014) Springer Nature]

Photographs of Ga₂O₃ thin films grown on a 50-mm diameter, single-side-polished (0001) sapphire substrate and a 200-mm (100) Si substrate are shown in Figure 6.

2.3 Growth of β-Ga₂O₃ thin films by ALD

ALD is a variant of CVD deposition, which is divided into a plasma-enhanced ALD (PE-ALD) and a more common thermal ALD. ALD is known for offering the capacity to control the thin film thickness and properties very precisely by reacting precursors sequentially and repetitively with the surface of the substrate instead of with each precursor. Such thin films can hence have reduced impurity content and pinhole density. In β -Ga₂O₃ thin film growth using ALD, Comstock and Elam reported that the oxygen precursor is limited to ozone ⁴⁹. H₂O₂, isopropanol, O₂, O₃ and H₂O/O₂ including water were used as oxygen precursors, but only ozone was effective. However, the possibility of growing β -Ga₂O₃ thin films by PE-ALD using O₂ plasma was also mentioned.

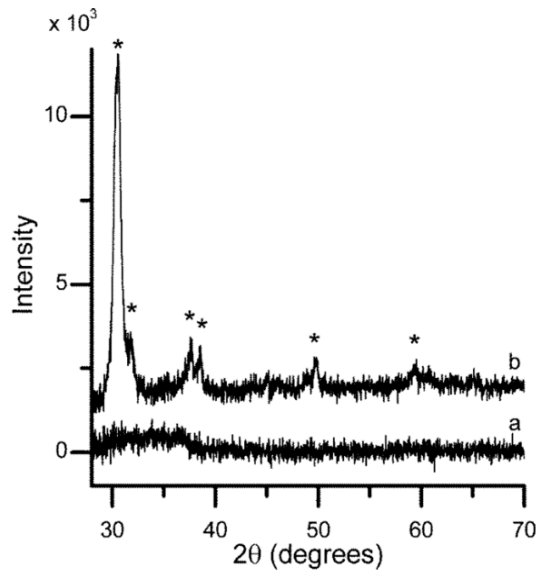


Figure 7. X-ray diffraction (XRD) data for an 800 Å thick Ga₂O₃ film deposited on fused SiO₂ with TMGa-O₃ at 350 °C. (a) Asdeposited, and (b) after annealing at 900°C under Ar. Diffraction peaks assigned to β-Ga₂O₃ are indicated by the star symbols. [Reprinted with permission from ⁴⁹ Copyright (2012) American Chemical Society.]

Figure 7 shows XRD 2 theta-omega scans for an ALD grown 800 Å thick Ga_2O_3 film before and after annealing at 900 °C under Ar. The XRD data, indicate that the Ga_2O_3 films were amorphous as-deposited but crystallized into the β- Ga_2O_3 phase upon annealing at 900 °C. The β- Ga_2O_3 thin film was stoichiometric, free of residual carbon and possessed properties similar to bulk β- Ga_2O_3 . Shan et al. studied the growth of Ga_2O_3 on Si (100) and sapphire (0001) substrates using O_2 plasma by PE-ALD ⁵⁰. [(CH₃)₂GaNH₂]₃ was used as a precursor for Ga and the growth temperature and pressure were 200°C and 3.0 Torr, respectively. The films annealed at 700°C or higher showed a (400) orientation, and the films grown on sapphire showed high optical transmittance below bandgap. Altuntas et al. reported on Ga_2O_3 grown on p-type Si (111) by PECVD using TMGa and an O_2 plasma ²¹. This study also showed that as-grown films were amorphous but crystallized into β- Ga_2O_3 after annealing under N_2 atmosphere at 700, 800 and 900 °C. The authors evaluated the leakage current densities, leakage current conduction mechanisms, dielectric constants, flat-band voltages, threshold voltages, and effective oxide charges of the capacitors as a function of annealing temperature.

2.4 Growth of β-Ga₂O₃ thin films by MBE

Many studies have reported on the growth of β -Ga₂O₃ thin films by MBE ^{7,16,23,51–54}. Normally, in order to grow doped β -Ga₂O₃, Ga and dopants such as Si or Sn are evaporated from Knudsen cells. For oxygen supply, radio frequency (RF)-activated radicals or a mixture of ozone and molecular oxygen gases were used. Most growth experiments were conducted between 600 and 900°C. In general, it has been reported that crack-free step-flow growth and smoother surface morphologies were promoted by lower growth temperatures ^{23,51}. The growth rate of β -Ga₂O₃ thin films was

found to vary significantly with substrate and growth temperature ^{51–53}. For example, Sasaki et al. found that the homoepitaxial growth rate was more than 10 times higher for the (310) or (010) planes than for the (100) plane ⁵¹.

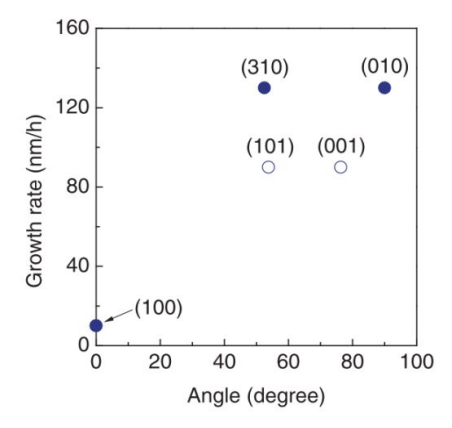


Figure 8. Relationship between surface orientation of β-Ga₂O₃ substrate and the homoepitaxial MBE growth rate. The horizontal axis is the angle between the substrate surface and (100) plane. [Copyright (2012) The Japan Society of Applied Physics.]

Figure 8 shows the relationship between surface orientation of the β -Ga₂O₃ substrate and the homoepitaxial growth rate. It is proposed that this is because the adhesion energy is lower on the (100) plane (as evidenced by a higher cleavability) than on the other planes. Indeed, it has also been reported by Oshima et al. that low growth rates due to a weak adhesion energy of the (100) plane can lead to step-flow growth ²³.

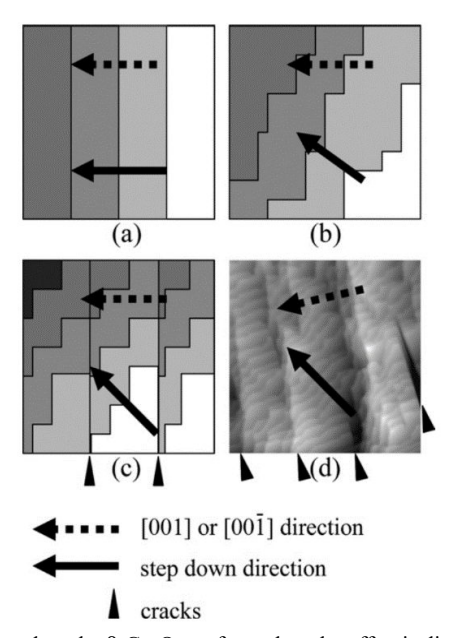


Figure 9. Models of step structures formed on the β-Ga₂O₃ surface when the off-axis direction is (a) along [001] or [00-1] and (b), (c) differs from [001] or [00-1]. An example of cracks observed by AFM is shown in (d). [Reprinted with permission from 23 Copyright (2008) Elsevier.]

The authors suggested models of step structures formed on the β -Ga₂O₃ surface as shown in Figure 9. The surface morphology is coherent with the fact that β -Ga₂O₃ is easily cleaved along the (100) and (001) planes. Straight steps are formed when the off-axis direction coincides with the [001] or [00-1] direction, and they lead to uniform step-flow on the

terraces, contributing to smooth surfaces, as shown in Figure 9 (a). The geometrical epitaxial relationship between β -Ga₂O₃ and a c-sapphire (0001) substrate is shown in Figure 10.

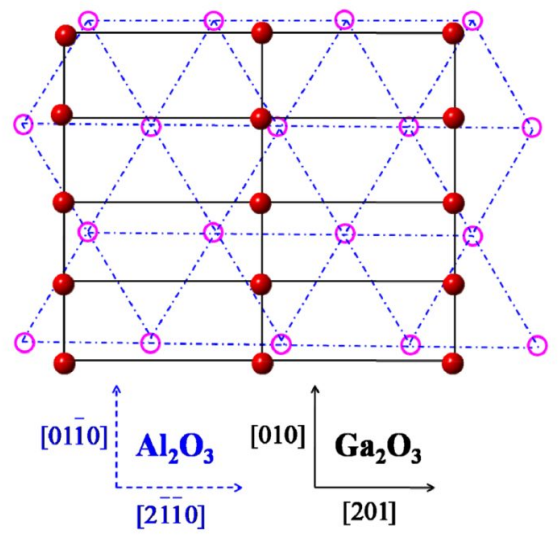


Figure 10. Schematic diagram of the epitaxial relationship between Al_2O_3 and β-Ga₂O₃ (-201). The lattices of film and substrate are deliberately offset for clarity. [Reprinted with permission from 53 , Optical Society of America.]

Guo and co-workers presented a schematic diagram of the crystallographic relationship between Al_2O_3 and β -Ga₂O₃ (-201) ⁵³. Generally, β -Ga₂O₃ thin films on c-sapphire substrates grow with preferential (-201) orientation. This is because the (-201) plane oxygen atom arrangement is the same as that for the β -Ga₂O₃ thin film and the c-sapphire substrate ^{52,53,55}

3. DOPING OF BETA-GALLIUM OXIDE THIN FILMS

In order to use the β -Ga₂O₃ thin film for electronic and optoelectronic devices, precise carrier concentration control by doping is required. Demonstration of the control of the electrical conductivity of β -Ga₂O₃ thin films by n-type impurity doping changed the research paradigm for β -Ga₂O₃ thin films. In this section we give an overview of the various approaches used to give high quality doping.

3.1 n-type doping

Group IV elements such as Si, Ge and Sn are commonly used as dopants to produce n-type electrical conductivity and control free electron concentration during β-Ga₂O₃ thin film growth. These dopants can substitute on the Ga site to form a shallow donor level. F and Cl can also act as shallow donors through substitutional doping at the O site 56. The first precise control of the carrier concentration through impurity doping was developed using homoepitaxial growth. Sasaki et al. reported MBE growth of a 0.7 μm thick Sn-doped β-Ga₂O₃ thin film on an Mg-doped semi-insulating (010) β-Ga₂O₃ substrate ⁵¹. Control of the carrier concentration over the range 10¹⁶–10¹⁹ cm⁻³ was achieved. Homoepitaxial Si and Sn doped β-Ga₂O₃ thin films were grown on a (010) β-Ga₂O₃ substrate without introduction of significant densities of dislocations or planar defects by Baldini et al 13. Tetraethylorthosilicate (TEOS) and tetraethyltin (TESn) were used as dopant precursors for Si and Sn, respectively. The growth of doped β-Ga₂O thin films was performed in a low-pressure MOCVD reactor with a vertical shower head. When Si was used as the dopant, the carrier concentration was controlled (from 10^{17} to 8 x 10^{19} cm⁻³) through the precursor flow rate. The authors observed, on the other hand, that the carrier concentration doping range was more limited (4×10^{17} to 10^{19} cm⁻³) when Sn doping was employed, and it was suggested that this may be due to a memory effect of Sn in the reactor. The measured electron mobility of the homoepitaxial β-Ga₂O₃ thin films with both dopants increased from ~50 cm²/Vs to ~130 cm²/Vs as the doping level decreased. Krishnamoorthy et al. demonstrated Si delta doping in β-Ga₂O₃ grown on (010) β-Ga₂O₃ substrates by PA-MBE using a shutter pulsing technique⁸. Hall measurements indicated a total charge of 2.4×10¹⁴ cm⁻² with a high mobility of 83 cm²/Vs and a sheet resistance of 320 Ω /sq. This relatively high mobility was explained to be a result of the electron population diffusing into the undoped β -Ga₂O₃ region, leading to less impurity scattering. Post-growth Siion implantation in β -Ga₂O₃ thin films has been studied by Sasaki et al ⁵⁷. The total dose was varied from $2x10^{14}$ to $2x10^{15}$ cm⁻², corresponding to Si concentrations from $1x10^{19}$ to $1x10^{20}$ cm⁻³. Si ion implanted Ga₂O₃ showed a high activation efficiency of above 60 % through annealing under N₂ atmosphere at 900–1000°C.

Doping experiments in heteroepitaxial β-Ga₂O₃ were also conducted, mainly using sapphire substrates. These could be attractive alternatives to native substrates for wider area/lower-cost growth of power electronics and SBPD devices. The growth of β-Ga₂O₃ doped with Si and Sn using c-sapphire was studied by Gogova and co-workers ^{15,26}. The authors used TEOS and TESn as precursors for Si and Sn, respectively. SIMS measurements revealed carrier concentration ranges of 4x10¹⁷– 5x10¹⁹ cm⁻³ and 10¹⁷–10¹⁸ cm⁻³ for Si and Sn-doping, respectively. However, in the Hall effect measurement of Si and Sn doped β-Ga₂O₃ thin films, no electrical conductivity could be confirmed. Annealing in O₂ was attempted in order to electrically activate the Si and Sn but the layers retained their semi-insulating characteristics. It was proposed that the low conductivity could come from compensation of the Si-donors and Sn-donor by dislocations and stacking faults (SFs). Furthermore, in the case of Si doping, it was mentioned that a SiO₂ parasite phase was present. The growth of Si doped β-Ga₂O₃ thin films on c-sapphire was demonstrated using LPCVD by Rafique et al ³⁶. SiCl₄ was used as an n-type dopant gas. Hall measurements at room temperature showed that the carrier concentration could be tuned from high-10¹⁶ to low-10¹⁹ cm⁻³ as a function of the SiCl₄ doping source flow rate. The highest electron Hall mobility at room temperature (of 42.35 cm²/Vs) was measured on a c-sapphire substrate for a carrier concentration 1.32x10¹⁸cm⁻³. Another paper also showing electrical conductivity using non-native substrates was reported by Mi et al ³⁷. The authors reported that Sn doped β-Ga₂O₃ thin films with different Sn concentrations were deposited on MgO (110) substrates by MOCVD. TESn was used as a precursor for Sn. As the Sn content was increased from 1 to 10%, the resistivity decreased rapidly. The lowest resistivity of 5.21x10⁻² Ωcm was obtained for 10% Sn doped β-Ga₂O₃ thin films. The carrier concentration and Hall mobility values were 3.71x10¹⁹ cm⁻³ and 3.35 cm²/Vs, respectively.

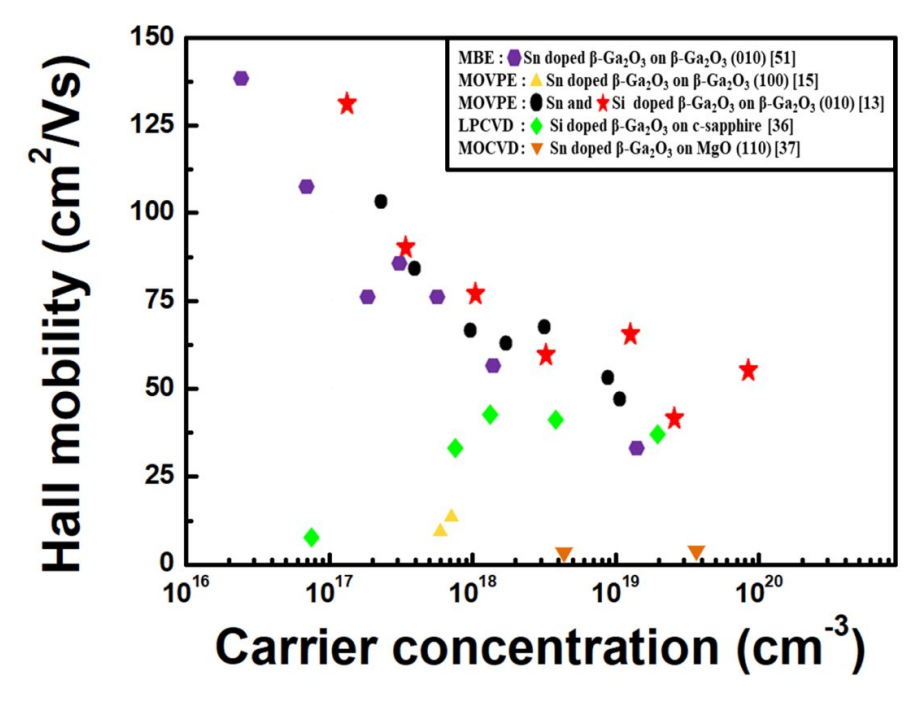


Figure 11. Summary of the Hall mobilities as a function of carrier concentration (log scale) for doped β -Ga₂O₃ thin films grown by various techniques.

Figure 11 shows a summary of the electrical properties of homo- and hetero-epitaxial doped β -Ga₂O₃ thin films. Although they generally showed lower mobilities than for homoepitaxial films, carrier concentration and mobility could, nevertheless, be controlled through impurity doping for heteroepitaxial layers.

3.2 p-type doping

A major drawback of β -Ga₂O₃ till present has been lack of a reliable method for fabricating p-type β -Ga₂O₃. This is a key limitation for its' entry into a whole range of semiconductor device markets.

Indeed, it is generally proposed that useful levels of majority acceptor (p-type) doping in β -Ga₂O₃ are unlikely to be obtained because of a combination of factors including the relatively low absolute energy level of the valence band, the lack of an identified shallow acceptor, the relatively high effective masses of holes at the top of the valence band, the propensity for self-trapping of holes and the relatively low formation energy of the oxygen vacancy donor which favors compensation of acceptors²⁹. Although, to the best of our knowledge, there are no direct demonstrations of impurity-doped p-type β -Ga₂O₃ in the literature several studies have, nevertheless, evoked the possibility of p-type doping. In 2005, Chang et al. synthesized β -Ga₂O₃ nanowires and introduced Zn as an acceptor by diffusion⁵⁸. The quasi one-dimensional carrier concentration and the mobility in the nanowires were estimated to be 5.3×10^8 cm⁻¹ and 3.5×10^{-2} cm²/Vs, respectively. These results were taken to demonstrate inherent carrier concentration and mobility limitations of p-type doping imposed by the relatively low valence band and the high effective masses expected for acceptors in β -Ga₂O₃. In addition to this study, there are other reports p-type doping of β -Ga₂O₃ nanowires using N₂ and NH₃ as sources of acceptors ^{59,60}. However, both studies only inferred p-type conduction from the IV curves and direct analysis of carrier type, concentration and mobility was not reported.

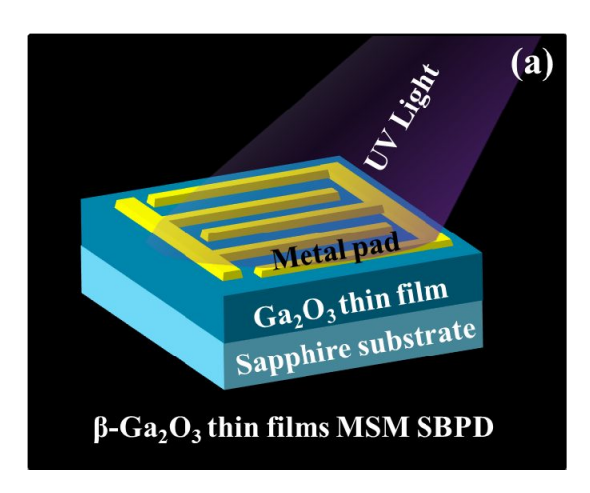
More recently Chikoidze et al. presented direct evidence of majority p-type conduction in nominally undoped β -Ga₂O₃ grown on c-sapphire substrates by pulsed laser deposition (PLD) (by the authors of this article) ⁶¹. Although the layers were relatively insulating at room temperature, majority hole conduction was established by high temperature Hall and Seebeck measurements. They were also comforted by findings from photoemission and cathodoluminescence spectroscopies. The ionization energy of the acceptor level was measured to be 1.1eV above the valence band edge. The gallium vacancy was identified as a possible acceptor candidate based on thermodynamic equilibrium Ga₂O₃ (crystal) - O₂ (gas) system calculations (Kroger theory) which revealed a window without oxygen vacancy compensation. Thus it was postulated that this p-type signal may have emerged thanks to the oxygen stoichiometry engineering possible with PLD allowing a reduction in oxygen vacancy compensation.

4. APPLICATIONS OF BETA-GALLIUM OXIDE THIN FILMS

Based on the various demonstrations of β -Ga₂O₃ epitaxial growth and n-type doping, it has been adopted in various fields such as gas sensors ^{62–65}, photoelectrodes for water splitting devices ^{66,67}, SBPD and FETs for power electronics and rf switching devices, etc. In particular, the state-of-the-art in device performance for certain SBPD operating wavelengths and some power electronic device architectures have been greatly advanced through the adoption β -Ga₂O₃ thin film technology. In this section, therefore, we give an overview of the current advances in β -Ga₂O₃ based SBPD and FETs.

4.1 Solar-blind UV photo detectors

In the past few decades compact solid state SBPDs have emerged for use in various fields such as fire detection, air purification, ozone hole monitoring, biological/chemical analysis, missile tracking, etc $^{68-70}$. The market is currently dominated by SiC-based devices. These rely on the use of filters in order to achieve solar blindness, however, so there has recently been a lot of interest in their replacement with devices based on WBG compound semiconductors with bandgaps that can be tuned into the UVC (> ~4.4eV) by alloying. In (Al)GaN and (Mg)ZnO (the two main candidates currently) for instance, increasing the proportion of Al and Mg (respectively) allows us to attain good SBPD operation. However, introducing higher Al and Mg contents deteriorates the quality of the thin films and causes phase segregation and progressive performance drop-off for operation further into the UVC 71,72 . Therefore, a conductive UWBG with a natural bandgap of 4.9eV (i.e. monoclinic β -Ga₂O₃) is an attractive choice for adoption as a new SPBD material $^{10,22,73-75}$.



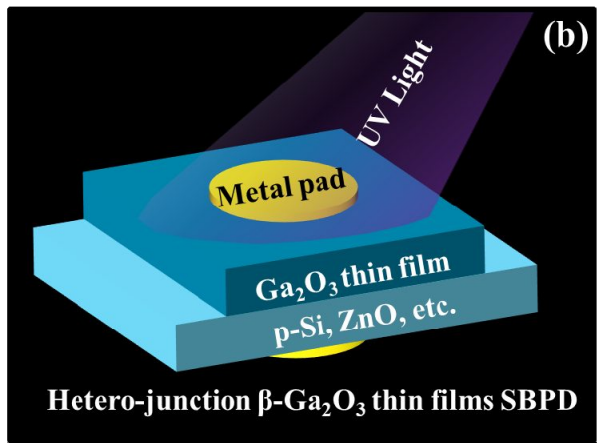


Figure 12. Schematic representation of (a) a typical β -Ga₂O₃ thin film MSM structure SBPD and (b) a β -Ga₂O₃ thin film based heterojunction SBPD.

The most common architecture of β -Ga₂O₃ thin films SBPD reported in the literature is the simple inter-digitated-transducer (IDT) metal-semiconductor-metal (MSM) structure (as shown in Figure 12 (a)) and most of the experiments were performed using sapphire substrates $^{11,22,52,73-78}$. Oshima et al. evaluated β -Ga₂O₃ MSM SBPD grown on c-sapphire substrates by PA-MBE 79 .

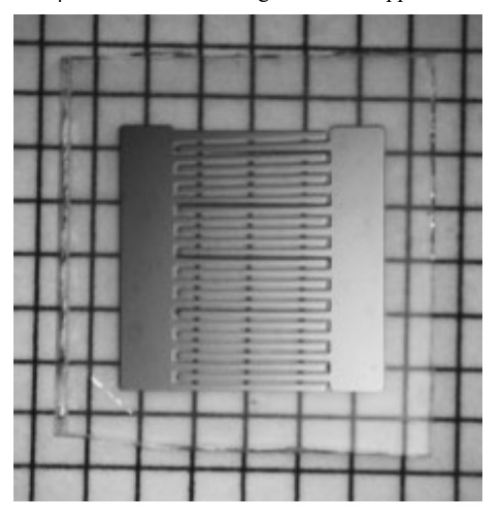


Figure 13. Photograph of a β-Ga₂O₃ based IDT MSM SBPD. [Copyright (2007) The Japan Society of Applied Physics.]

The MSM shown in Figure 13 consists of 12 pairs of fingers with lengths of 3 mm and finger widths/spacings of 100 μ m. The electrodes consist of Au (100 nm)/Ti (50 nm) bilayers which were deposited through a shadow mask by vacuum evaporation. The device showed a small dark current of 1.2 nA at 10V. The responsivity and external quantum efficiency (EQE) were 0.037 A/W and 18 % (under 254 nm light illumination) respectively. The relatively low dark current and good responsivity/EQE indicated much promise for future development. As β -Ga₂O₃ thin film growth technology has advanced, the performance of β -Ga₂O₃ based SBPD has increased rapidly. Wuu et al. fabricated MSM SBPD using β -Ga₂O₃ thin film grown on c-sapphire substrates by MOCVD ⁸⁰. The maximum responsivity was 20.1 A/W at 260 nm with an applied voltage of 5V. Hu and co-workers also designed and fabricated Au/ β -Ga₂O₃ IDT SBPD ²⁷. The responsivity and EQE (with an applied voltage of 20 V) were 17 A/W and 8228 % respectively. These high values were attributed to the Au electrode providing a carrier multiplication region. Liu et al. reported even higher values for spectral responsivity and EQE of 259 A/W and 7.9x10⁴ %, respectively⁵². To better understand the optical properties of Ga₂O₃, we (the authors of this article) measured two-color time resolved differential transmission (TRDT) using Ga₂O₃ thin films with different growth temperatures (610 ~ 690 °C):

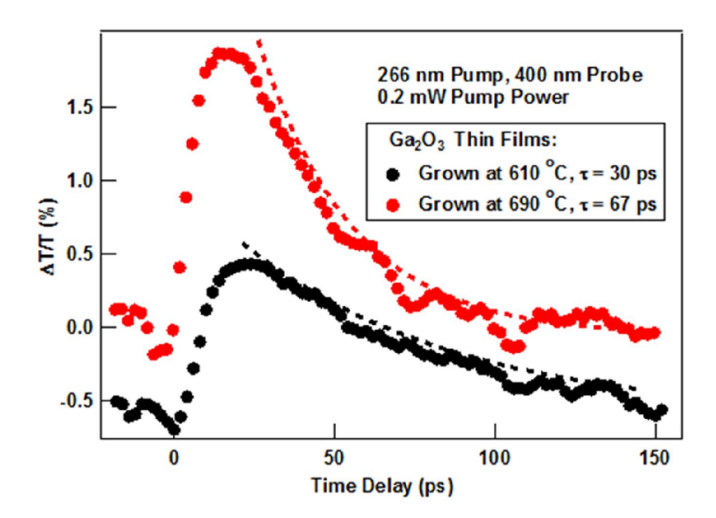


Figure 14. Two color pump/probe measurements show an initial increase in TRDT followed by a recovery toward equilibrium over a time scale of 30-70 ps for the samples. The exponential fits are shifted for clarity.

As shown in Figure 14 (a), the TRDT show an initial increase after the excitation at 266 nm followed by a gradual decline. It was found that this decay could be modeled by a single exponential fit, and the time constant, τ, was coherent with a relaxation of photo-excited carriers toward the equilibrium ^{81–83}. A much larger change in the photo-induced differential transmission was observed for the sample grown at 690 °C. It was postulated that this may be due to the higher crystal quality and smoother surface morphology obtained at higher temperature. SBPD were made from the higher temperature (690°C) layers using a simple MSM IDT structure. Spectral responsivity studies revealed a peak at 261 nm and a maximum EQE of 41.7% for a -2.5 V bias. I/V curves, both with and without Xenon back-illumination, revealed a photocurrent about 3 orders of magnitude higher than the dark current for a bias of -2.5 V. Recently, several groups have reported improving the performance of β -Ga₂O₃ MSMs by doping (with, for example. Si, Sn, Zn etc.) ^{73,76,77,83}. For example, β -Ga_{2-x}Sn_xO₃ thin films on c-sapphire substrates were deposited with different Sn contents by Zhao et al ⁷⁴. The author attributed an improvement in MSM performance to the presence of Sn⁴⁺ ions in the β-Ga₂O₃ films. Alema et al. fabricated β-Ga₂O₃:Zn/β-Ga₂O₃ thin films on c-sapphire substrates for SBPD evaluation ⁷⁷. In asgrown β-Ga₂O₃:Zn/β-Ga₂O₃ thin films the resulting MSM SBPDs showed a strong responsivity (linked to a high density of internal defects) of > 10³ A/W. The responsivity in MSM SBPD based on the same films after post-growth thermal annealing was found to fall to 210 A/W (with a peak response at 232 nm). In addition to studying the performance improvement of β-Ga₂O₃ SBPD by doping, research on β-Ga₂O₃ thin films SBPD using heterojunctions such as β-Ga₂O₃/GaN, β-Ga₂O₃/ZnO, β-Ga₂O₃/p-Si, etc is also being conducted. A schematic illustration of a typical β-Ga₂O₃ thin film-based hetero-junction SBPD is shown in Figure 12 (b). Guo and co-workers reported zero power consumption SBPDs based on β -Ga₂O₃/NSTO (NSTO = Nb:SrTiO₃) and β -Ga₂O₃/ZnO heterojunctions ^{10,85}. β -Ga₂O₃/NSTO and β - Ga_2O_3/ZnO heterojunctions SBPD with zero bias showed I_{photo}/I_{dark} ratios of ≈ 20 and ~ 14.8 , respectively, under 254 nm illumination (of 45 μW/cm² and 50 μW/cm² in intensity, respectively). In addition to these results, SBPD comprised of β-Ga₂O₃/GaN Schottky barriers were shown to have controllable depletion depths and thus switched operating mode between solar-blind and visible-blind by simply changing the applied bias⁸⁶. SBPD comprised of β-Ga₂O₃ films on p-Si (100) substrates showed relatively high responsivities and EQEs of 370 A/W and 1.8x10⁵ % respectively³⁰. Extension of the β-Ga₂O₃ photodetector operating wavelength range has been investigated based on the β-(AlGaIn)₂O₃ alloy system ^{11,76}. According to these studies, the detection range was tunable from 238 nm to 315 nm depending on the proportion of Al and In in the β-Ga₂O₃ thin films. In a different way, An et al. demonstrated UV (254 nm) + visible (510 nm) photodetection through Au plasmon enhanced β-Ga₂O₃ thin film SBPD ¹². Wu et al. suggested the possibility of fabricating UV detection + NIR luminescence application devices through Er³⁺-doped β-Ga₂O₃ thin films ⁷⁸. Table 2 summarizes the photoresponse parameters reported recently for some β-Ga₂O₃ thin film based SBPDs.

Materials	Substrate	Responsivity [AW-1]	EQE [%]	Ref.
β-Ga ₂ O ₃ thin film	c-sapphire	20.1 (260 nm)	-	80
β -Ga ₂ O ₃ thin film	c-sapphire	3.3 (236 nm)	-	75
$\beta\text{-}Ga_2O_3 \text{ thin film}$	c-sapphire	0.037 (254 nm)	18	79
$\beta\text{-}Ga_2O_3$ thin film	c-sapphire	54.9 (254 nm)	-	22
$\beta\text{-}Ga_2O_3$ thin film	c-sapphire	0.058 (259 nm)	28.3	73
$\beta\text{-}Ga_2O_3 \text{ thin film}$	c-sapphire	259 (235 nm)	7.9×10^4	52
Ga ₂ O ₃ thin film	c-sapphire	0.09 (261 nm)	41.7	Our work
$\beta\text{-}Ga_2O_3$ thin film	a-sapphire	17 (255 nm)	8228	27
$\beta\text{-}Ga_2O_3$ thin film	p-Si (100)	370 (254 nm)	1.8x10 ⁵	30
$\beta\text{-}Ga_2O_3$ thin film	ZnO	0.35 (254 nm)	1.7×10^2	85
$\beta\text{-}Ga_2O_3$ thin film	NSTO	43.31 (254 nm)	2.1×10^4	10
$\beta\text{-}(In_xGa_{1\text{-}x})_2O_3$ thin film	c-sapphire	30 (250nm)	-	76
$\beta\text{-}(Al_xGa_{1\text{-}x})_2O_3$ thin film	c-sapphire	1.5 (243 nm)	783	11
Si doped $\beta\text{-}Ga_2O_3$ thin film	c-sapphire	1.45 (254 nm)	-	84
Zn doped β -Ga ₂ O ₃ thin film	c-sapphire	210 (232 nm)	-	77
Sn doped β-Ga ₂ O ₃ thin film	c-sapphire	3.61x10 ⁻² (254 nm)	-	74

Table 2. Summary of the photoresponse parameters for $\beta\text{-}Ga_2O_3$ thin film based SBPD.

4.2 Field effect transistors

Table 3 compares intrinsic β -Ga₂O₃ material properties to those of other major WBG semiconductors. Of particular note is the breakdown field which is about 8 MV/cm. Combined with the propensity for n-type conduction through impurity-doping (see section 3 above) this high value of breakdown field makes β -Ga₂O₃ highly attractive for use in FET based power electronics. The initial stage of FET device development using β -Ga₂O₃ thin films was difficult due to the absence

of native substrates. Comparatively small Hall mobility (0.44 cm²/Vs) and field effect mobility (5x10⁻² cm²/Vs) were measured in early-stage FET studies using β -Ga₂O₃ thin films fabricated on sapphire substrates ⁸⁷. β -Ga₂O₃ based FET performance then soared when high quality wide-area β -Ga₂O₃ native substrates (produced by melt growth) became available ^{88–95}.

Materials	GaN	4H-SiC	diamond	β-Ga ₂ O ₃
Band gap E _g (eV)	3.4	3.3	5.5	~ 4.9
Breakdown field E _b (MV/cm)	3.3	2.5	10	8
Electron mobility μ (cm ² /Vs)	1200	1000	2000	300
Thermal conductivity (W/mK) ⁹⁶	210	270	1000	13 [100]
Thermal conductivity (w/mx)		270		23 [010]

Table 3. Intrinsic properties of major WBG semiconductor materials.

Higashiwaki et al. fabricated circular MESFETs using Sn-doped β -Ga₂O₃ thin films on Mg-doped semi-insulating β -Ga₂O₃ (010) substrates by MBE ¹⁶. The substrate was fabricated by the floating zone (FZ) method and SnO₂ powder was used as a source for the thin film doping. Ohmic metal contacts were formed using evaporated Ti(20 nm)/Au(230 nm) bilayers and contact resistance was significantly reduced by reactive ion etching (RIE) surface treatment before metal contact deposition. Pt(15 nm)/Ti(5 nm)/Au(250 nm) layers were used as Schottky gate contacts. The fabricated MESFETs exhibited excellent DC device characteristics with a drain current modulated by the gate voltage, a perfect pinch-off of the drain current, an off-state breakdown voltage over 250 V, a high on/off drain current ratio of around 10⁴, and a small gate leakage current. Higashiwaki and co-workers also reported depletion mode β-Ga₂O₃ thin film MOSFETs using Si ion implantation ⁹⁷. Fe-doped semi-insulating β-Ga₂O₃ (010) substrates fabricated by the FZ method were used and a 300 nm thick Sn doped β-Ga₂O₃ n-channel layer with a carrier concentration of 7x10¹⁷ cm⁻³ was grown by MBE. Figure 15 shows (a) a schematic cross-section of the device and (b) a top-view optical micrograph of the fabricated depletion-mode Ga₂O₃ MOSFET.

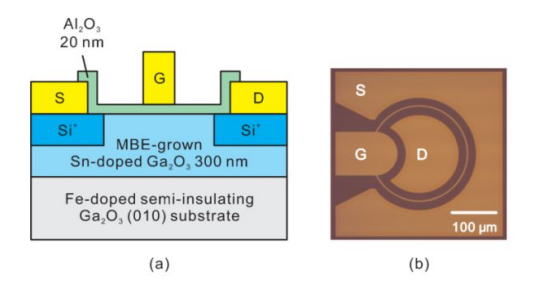


Figure 15. (a) Schematic cross-section and (b) optical micrograph of the fabricated depletion-mode Ga₂O₃ MOSFET. [Reprinted with permission from ⁹⁶ Copyright (2013) AIP Publishing LLC.]

Si-ion implantation doping was performed to the source and drain electrode regions in order to obtain low-resistance ohmic contacts. The contact resistance of the source and drain was reduced by RIE surface pre-treatment. Ti(20 nm) and Au(230 nm) layers were deposited by thermal evaporation. Al_2O_3 films formed by ALD were used to form the gate

dielectric and passivate the device surface (and thus significantly reduce gate leakage). The gate metal was formed from Ti(3 nm)/Pt(12 nm)/Au(280 nm) layers deposited on top of the Al_2O_3 film. The fabricated MOSFET showed good characteristics with a maximum I_d of 39 mA/mm (for a V_g of +4V), an on-off ratio of >10¹⁰ and a three-terminal V_{br} of 370 V. The device was found to maintain performance without significant permanent degradation up to an operating temperature of 250 °C.

 β -Ga₂O₃ thin film MOSFETs formed on non-native substrates have also been reported. Tadjer et al. fabricated MOSFETs using Si implanted β -Ga₂O₃ thin films grown on sapphire substrates by MOCVD ⁴⁴. Si-ion implantation was selectively performed only in the source and drain regions in order to fabricate a normally-off operation device. Ti(20 nm)/Au(200 nm) bilayers were deposited on the source and drain regions in order to form ohmic contacts and Al₂O₃ was deposited as the gate dielectric using ALD. The device showed that is was possible to fabricate a β -Ga₂O₃ MOSFET using a non-native substrate but it exhibited a relatively low maximum drain current of 42 nA at 100 V due to very high sheet and contact resistances. A homoepitaxial β -Ga₂O₃ thin film MOSFET with a very similar structure was described by Wong et al ⁷.

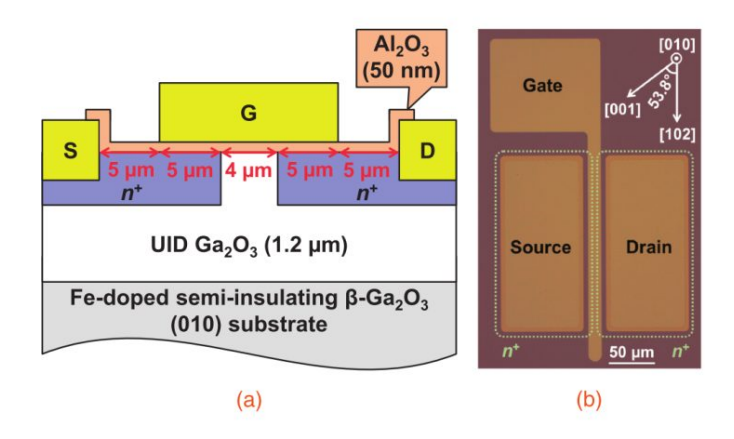


Figure 16. (a) Schematic cross section and (b) optical micrograph of the enhancement-mode β -Ga₂O₃ (010) MOSFET with Si⁺-implanted source/drain contacts and access regions. The dotted boundaries in (b) enclose the Si⁺-implanted n⁺ areas that were separated by a channel length of 4 μ m. [Copyright (2017) The Japan Society of Applied Physics.]

Figure 16 shows (a) a schematic cross section and (b) an optical micrograph of the enhancement-mode β -Ga₂O₃ (010) MOSFET with Si⁺-implanted source/drain contacts and access regions. The dotted boundaries in (b) enclose the Si⁺-implanted n⁺ areas that were separated by a channel length of 4 μm. As shown in Figure 16 (a) a UID Ga₂O₃ thin film was grown on an Fe-doped semi-insulating β -Ga₂O₃ (010) substrate by MBE and n⁺ source/drain Ohmic and access regions were selectively doped by selective-area Si⁺ implantation. Ohmic contacts were formed with Ti(20 nm)/Au(230 nm) bilayers and a 50 nm thick Al₂O₃ was used as the gate dielectric. Ti(3 nm)/ Pt(12 nm)/Au(280 nm) layers were deposited on the gate electrode. Despite the relatively low carrier concentration (4x10¹⁴ cm⁻³) in the UID Ga₂O₃ a maximum I_{DS} of 1.4 mA/mm was measured. A high I_{on}/I_{off} ratio of ~ 10⁶ was achieved. β-Ga₂O₃ based FET technology has developed very rapidly, and research on fin array FETs (finFETs) was reported by Chabak et al ¹⁷. The devices were fabricated from a 300 nm thick Sn-doped β-Ga₂O₃ thin film grown homoepitaxially by MOCVD on a 100 mm² Mg-doped semi insulating (100) β-Ga₂O₃ substrate. Figure 17 shows (a) the fabrication process for the Ga₂O₃ finFETs and (b) an SEM image of a fabricated L_{SD} = 4 μm finFET revealing the geometry of the Ga₂O₃ fin channels and contacts.

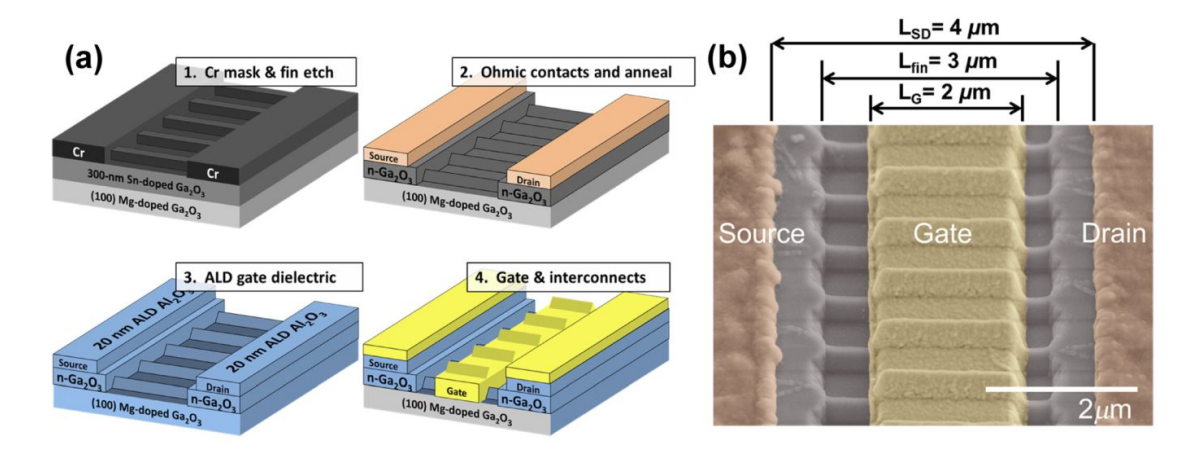


Figure 17. (a) Fabrication process for Ga_2O_3 finFETs and (b) a tilted false-colored SEM image of a L_{SD} = 4 μ m finFET depicting the geometry of Ga_2O_3 fin channels and contacts. [Reprinted with permission from ¹⁷ Copyright (2016) AIP Publishing LLC.]

Ti/Al/Ni/Au (20/100/50/50nm) contacts were formed on the source and drain. Rapid thermal annealing (1 min at 470 °C in nitrogen) was used to improve Ohmicity. A 20-nm Al₂O₃ gate dielectric was deposited at 250°C by ALD and patterned using fluorine-based RIE in order to make Ni/Au (20/480 nm) interconnects with an ~ 2 μm long optical gate metal evaporation. Despite I_{on} limitations, the finFET had a >10⁵ I_{on}/I_{off} ratio and (with an L_{GD} of 16 μm) showed the highest breakdown voltage of 612 V for a V_{GS} = 0 V off state. Krishnamoorthy et al used Si delta doped β-Ga₂O₃ in a MOSFET in order to realize high current density/mobility/frequency devices ⁸. The Si delta doped β-Ga₂O₃ was grown on Fe doped semi-insulating (010)-oriented β-Ga₂O₃ substrates by PA-MBE using a shutter pulsing technique. Silicon delta-doped layers were separated by 4 nm undoped Ga_2O_3 layers. Ohmic contacts were formed from Ti/Au/Ni layers with annealing at 470 °C for 1 min after deposition. A contact resistance of 0.35 Ω mm with a low specific resistance of 4.3 × 10⁻⁶ Ω cm² was measured using transfer length measurement (TLM) structures. The β-Ga₂O₃ thin films showed a very high electron mobility of ~80 cm²/Vs. The authors thus suggested that delta-doped layers can be used as excellent contact layers. Figure 18 shows (a) a device schematic and (b) output characteristics for the delta-doped FET device.

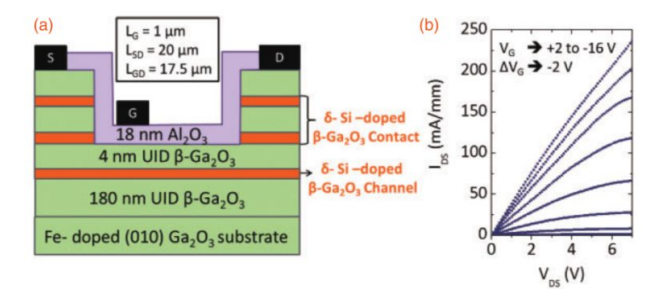


Figure 18. (a) Device schematic, (b) output characteristics of delta-doped FET device. [Copyright (2017) The Japan Society of Applied Physics.]

A 18 nm Al_2O_3 film was deposited as a gate dielectric by ALD, and Pt/Au/Ni layers were formed on the Al_2O_3 film by thermal evaporation. As can be seen in Figure 18 (b), a very high drain current maximum (I_D ,max) of 236 mA/mm was measured for a V_{DS} of 7 V and a V_G of +2 V. A three-terminal off-state breakdown voltage of 51 V (for $V_{GS} = -16$ V and V_{DS} , V_{DS} was measured for the device. V_{DS} nanostructure MOSFETs were also fabricated on V_{DS} substrates V_{DS} . The authors claimed that this interesting device design, fabricated by transfer of V_{DS} nanostructures

onto foreign substrates, can provide clues to overcome the poor thermal conductivity limitations of β -Ga₂O₃. It can be seen, therefore, that research on β -Ga₂O₃ FETs is proceeding rapidly and new possibilities are opening up thanks to the recent emergence of high quality epitaxy of impurity doped β -Ga₂O₃ thin films on non-native substrates.

5. CONCLUSIONS AND FUTURE PROSPECTS

In conclusion, we reviewed the state-of-the-art in β -Ga₂O₃ thin film growth and doping before giving an overview of the surge in exploration of β -Ga₂O₃ based UV photodetectors and FET-based power devices that has been observed over the past decade. It was explained that this boom in β -Ga₂O₃ research was driven partly by the availability of wide area single crystal β -Ga₂O₃ substrates and partly by a rapid development of high quality homoepitaxy and n-type impurity doping know-how. In addition to growth on native β -Ga₂O₃ substrates, it was shown that research into β -Ga₂O₃ thin films grown on non-native substrates has also been evolving rapidly with recent significant advances in doping control and high-quality epitaxy allowing demonstration of impressive SBPD and FETs on non-native substrates. Despite these various studies, there is still a long way to go before β -Ga₂O₃ penetrates real world UVC photodetector and power device markets. The authors propose that the following may be important research and development paths towards widespread market adoption of β -Ga₂O₃ thin film based devices.

- 1. Continued development of high quality homoepitaxial β-Ga₂O₃ thin film growth and doping technology using native substrates.
- 2. Native substrate cost reduction through scale-up of production volumes and wafer size.
- 3. Heteroepitaxial growth of high-quality β-Ga₂O₃ thin films on non-native substrates using an optimized buffer layer and/or new growth methods.
- Development of heterojunction-based applications/devices exploiting β-(Al_xGa_{1-x})₂O₃/β-Ga₂O₃ 2DEGs (e.g. HEMTs).
- 5. Emergence of novel doping approaches and related devices/applications (e.g. p-type doping for complementary metal—oxide–semiconductor (CMOS) circuitry or UV avalanche PD, etc.)
- 6. New concepts and designs to improve the thermal management and reliability of power electronics devices

Acknowledgement

This material is based upon work supported by the National Science Foundation under Grant No. ECCS-1748339

6. REFERENCES

- [1] Roy, R., Hill, V. G. and Osborn, E. F., "Polymorphism of Ga₂O₃ and the System Ga₂O₃—H₂O," J. Am. Chem. Soc. **74**(3), 719–722 (1952).
- [2] Marezio, M. and Remeika, J. P., "Bond Lengths in the α-Ga 2 O 3 Structure and the High-Pressure Phase of Ga 2– x Fe x O 3," J. Chem. Phys. **46**(5), 1862–1865 (1967).
- [3] Åhman, J., Svensson, G. and Albertsson, J., "A reinvestigation of β-gallium oxide," Acta Crystallogr. Sect. C Cryst. Struct. Commun. **52**(6), 1336–1338 (1996).

- [4] Otero Areán, C., López Bellan, A., Peñarroya Mentruit, M., Rodríguez Delgado, M. and Turnes Palomino, G., "Preparation and characterization of mesoporous γ-Ga₂O₃," Microporous Mesoporous Mater. **40**, 35–42 (2000).
- [5] Mezzadri, F., Calestani, G., Boschi, F., Delmonte, D., Bosi, M. and Fornari, R., "Crystal structure and ferroelectric properties of ε-Ga₂O₃ films grown on (0001)-sapphire," Inorg. Chem. **55**(22), 12079–12084 (2016).
- [6] Playford, H. Y., Hannon, A. C., Barney, E. R. and Walton, R. I., "Structures of uncharacterised polymorphs of gallium oxide from total neutron diffraction," Chem. A Eur. J. 19(8), 2803–2813 (2013).
- [7] Wong, M. H., Nakata, Y., Kuramata, A., Yamakoshi, S. and Higashiwaki, M., "Enhancement-mode Ga₂O₃ MOSFETs with Si-ion-implanted source and drain," Appl. Phys. Express **10**, 41101 (2017).
- [8] Krishnamoorthy, S., Xia, Z., Bajaj, S., Brenner, M. and Rajan, S., "Delta-doped β-gallium oxide field-effect transistor," Appl. Phys. Express 10, 51102 (2017).
- [9] Zhou, H., Si, M., Alghamdi, S., Qiu, G., Yang, L. and Ye, P. D., "High-Performance Depletion / Enhancement- Mode β-Ga₂O₃ on Insulator (GOOI) Field-Effect Transistors With Record Drain Currents of 600 / 450 mA / mm," IEEE Electron Device Lett. **38**(1), 103–106 (2017).
- [10] Guo, D., Liu, H., Li, P., Wu, Z., Wang, S., Cui, C., Li, C. and Tang, W., "Zero-Power-Consumption Solar-Blind Photodetector Based on β-Ga₂O₃/NSTO Heterojunction," ACS Appl. Mater. Interfaces **9**(2), 1619–1628 (2017).
- [11] Feng, Q., Li, X., Han, G., Huang, L., Li, F., Tang, W., Zhang, J. and Hao, Y., "(AlGa)₂O₃ solar-blind photodetectors on sapphire with wider bandgap and improved responsivity," Opt. Mater. Express 7, 1240–1248 (2017).
- [12] An, Y., Chu, X., Huang, Y., Zhi, Y., Guo, D., Li, P., Wu, Z. and Tang, W., "Au plasmon enhanced high performance β-Ga₂O₃ solar-blind photo-detector," Prog. Nat. Sci. Mater. Int. **26**, 65–68 (2016).
- [13] Baldini, M., Albrecht, M., Fiedler, A., Irmscher, K., Schewski, R. and Wagner, G., "Editors' Choice—Si- and Sn-Doped Homoepitaxial β-Ga₂O₃ Layers Grown by MOVPE on (010)-Oriented Substrates," ECS J. Solid State Sci. Technol. **6**, Q3040–Q3044 (2017).
- [14] Baldini, M., Albrecht, M., Fiedler, A., Irmscher, K., Klimm, D., Schewski, R. and Wagner, G., "Semiconducting Sn-doped β-Ga₂O₃ homoepitaxial layers grown by metal organic vapour-phase epitaxy," J. Mater. Sci. **51**, 3650–3656 (2016).
- [15] Gogova, D., Schmidbauer, M. and Kwasniewski, A., "Homo- and heteroepitaxial growth of Sn-doped β-Ga₂O₃ layers by MOVPE," CrystEngComm **17**, 6744–6752 (2015).
- [16] Higashiwaki, M., Sasaki, K., Kuramata, A., Masui, T. and Yamakoshi, S., "Gallium oxide (Ga₂O₃) metal-semiconductor field-effect transistors on single-crystal β-Ga₂O₃ (010) substrates," Appl. Phys. Lett. **100**, 13504 (2012).
- [17] Chabak, K. D., Moser, N., Green, A. J., Walker, D. E., Tetlak, S. E., Heller, E., Crespo, A., Fitch, R., McCandless, J. P., Leedy, K., Baldini, M., Wagner, G., Galazka, Z., Li, X. and Jessen, G., "Enhancement-mode Ga2O3 wrap-gate fin field-effect transistors on native (100) β-Ga₂O₃ substrate with high breakdown voltage," Appl. Phys. Lett. **109**, 1–6 (2016).
- [18] Hwang, W. S., Verma, A., Peelaers, H., Protasenko, V., Rouvimov, S., Xing, H., Seabaugh, A., Haensch, W., De Walle, C. Van, Galazka, Z., Albrecht, M., Fornari, R. and Jena, D.,

- "High-voltage field effect transistors with wide-bandgap β -Ga₂O₃ nanomembranes," Appl. Phys. Lett. **104**, 203111 (2014).
- [19] Rafique, S., Han, L. and Zhao, H., "Synthesis of wide bandgap Ga₂O₃(E g ~ 4.6-4.7 eV) thin films on sapphire by low pressure chemical vapor deposition," Phys. Status Solidi **213**, 1002–1009 (2016).
- [20] Hu, D., Zhuang, S., Ma, Z., Dong, X., Du, G., Zhang, B., Zhang, Y. and Yin, J., "Study on the optical properties of β-Ga₂O₃ films grown by MOCVD," J. Mater. Sci. Mater. Electron. 28(15), 10997–11001 (2017).
- [21] Altuntas, H., Donmez, I., Ozgit-Akgun, C. and Biyikli, N., "Effect of postdeposition annealing on the electrical properties of β-Ga₂O₃ thin films grown on p-Si by plasmaenhanced atomic layer deposition," J. Vac. Sci. Technol. A **32**, 41504 (2014).
- [22] Qian, L.-X., Zhang, H.-F., Lai, P. T., Wu, Z.-H. and Liu, X.-Z., "High-sensitivity β-Ga₂O₃ solar-blind photodetector on high-temperature pretreated c-plane sapphire substrate," Opt. Mater. Express 7(10), 3643–3653 (2017).
- [23] Oshima, T., Arai, N., Suzuki, N., Ohira, S. and Fujita, S., "Surface morphology of homoepitaxial β-Ga2O3 thin films grown by molecular beam epitaxy," Thin Solid Films **516**(17), 5768–5771 (2008).
- [24] Liu, G. X., Shan, F. K., Lee, W. J., Shin, B. C., Kim, S. C., Kim, H. S. and Cho, C. R., "Growth temperature dependence of Ga₂O₃ thin films deposited by plasma enhanced atomic layer deposition," Integr. Ferroelectr. **94**, 11–20 (2007).
- [25] Nomura, K., Goto, K., Togashi, R., Murakami, H., Kumagai, Y., Kuramata, A., Yamakoshi, S. and Koukitu, A., "Thermodynamic study of β-Ga₂O₃ growth by halide vapor phase epitaxy," J. Cryst. Growth **405**, 19–22 (2014).
- [26] Gogova, D., Wagner, G., Baldini, M., Schmidbauer, M., Irmscher, K., Schewski, R., Galazka, Z., Albrecht, M. and Fornari, R., "Structural properties of Si-doped β-Ga₂O₃ layers grown by MOVPE," J. Cryst. Growth **401**, 665–669 (2014).
- [27] Hu, G. C., Shan, C. X., Zhang, N., Jiang, M. M., Wang, S. P. and Shen, D. Z., "High gain Ga₂O₃ solar-blind photodetectors realized via a carrier multiplication process," Opt. Express **23**, 13554 (2015).
- [28] Sbrockey, N. M., Salagaj, T., Coleman, E., Tompa, G. S., Moon, Y. and Kim, M. S., "Large-Area MOCVD Growth of Ga₂O₃ in a Rotating Disc Reactor," J. Electron. Mater. **44**(5), 1357–1360 (2015).
- [29] Mastro, M. A., Kuramata, A., Calkins, J., Kim, J., Ren, F. and Pearton, S. J., "Perspective— Opportunities and Future Directions for Ga₂O₃," ECS J. Solid State Sci. Technol. 6, P356– P359 (2017).
- [30] Guo, X. C., Hao, N. H., Guo, D. Y., Wu, Z. P., An, Y. H., Chu, X. L., Li, L. H., Li, P. G., Lei, M. and Tang, W. H., "β-Ga₂O₃/p-Si heterojunction solar-blind ultraviolet photodetector with enhanced photoelectric responsivity," J. Alloys Compd. 660, 136–140 (2016).
- [31] Kong, L., Ma, J., Luan, C., Mi, W. and Lv, Y., "Structural and optical properties of heteroepitaxial beta Ga₂O₃ films grown on MgO (100) substrates," Thin Solid Films **520**(13), 4270–4274 (2012).
- [32] Kaneko, K., Ito, H., Lee, S. D. and Fujita, S., "Oriented growth of beta gallium oxide thin films on yttrium-stabilized zirconia substrates," Phys. Status Solidi **10**, 1596–1599 (2013).

- [33] Binions, R., Carmalt, C. J., Parkin, I. P., Pratt, K. F. E. and Shaw, G. A., "Gallium oxide thin films from the atmospheric pressure chemical vapor deposition reaction of gallium trichloride and methanol," Chem. Mater. 16, 2489–2493 (2004).
- [34] Terasako, T., Ichinotani, H. and Yagi, M., "Growth of β-gallium oxide films and nanostructures by atmospheric- pressure CVD using gallium and water as source materials," Phys. Status Solidi Curr. Top. Solid State Phys. 12, 985–988 (2015).
- [35] Rafique, S., Han, L., Tadjer, M. J., Freitas, J. A., Mahadik, N. A. and Zhao, H., "Homoepitaxial growth of β-Ga₂O₃ thin films by low pressure chemical vapor deposition," Appl. Phys. Lett. **108**, 182105 (2016).
- [36] Rafique, S., Han, L., Neal, A. T., Mou, S., Tadjer, M. J., French, R. H. and Zhao, H., "Heteroepitaxy of N-type β-Ga₂O₃ thin films on sapphire substrate by low pressure chemical vapor deposition," Appl. Phys. Lett. **109**, 132103 (2016).
- [37] Mi, W., Du, X., Luan, C., Xiao, H. and Ma, J., "Electrical and optical characterizations of β-Ga₂O₃: Sn films deposited on MgO (110) substrate by MOCVD," RSC Adv. 4, 30579 (2014).
- [38] Boschi, F., Bosi, M., Berzina, T., Buffagni, E., Ferrari, C. and Fornari, R., "Hetero-epitaxy of ε-Ga₂O₃ layers by MOCVD and ALD," J. Cryst. Growth **443**, 25–30 (2016).
- [39] Feng, X., Li, Z., Mi, W. and Ma, J., "Effect of annealing on the properties of Ga₂O₃:Mg films prepared on α-Al₂O₃ (0001) by MOCVD," Vacuum **124**, 101–107 (2016).
- [40] Ravadgar, P., Horng, R. H. and Wang, T. Y., "Healing of Surface States and Point Defects of Single-Crystal β-Ga₂O₃ Epilayers," ECS J. Solid State Sci. Technol. **1**(4), 58–60 (2012).
- [41] Lv, Y., Ma, J., Mi, W., Luan, C., Zhu, Z. and Xiao, H., "Characterization of β-Ga₂O₃ thin films on sapphire (0001) using metal-organic chemical vapor deposition technique," Vaccum **86**, 1850–1854 (2012).
- [42] Huang, C.-Y., Horng, R.-H., Wuu, D.-S., Tu, L.-W. and Kao, H.-S., "Thermal annealing effect on material characterizations of β-Ga₂O₃ epilayer grown by metal organic chemical vapor deposition," Appl. Phys. Lett. **102**, 11119 (2013).
- [43] Wagner, G., Baldini, M., Gogova, D., Schmidbauer, M., Schewski, R., Albrecht, M., Galazka, Z., Klimm, D. and Fornari, R., "Homoepitaxial growth of β-Ga₂O₃ layers by metal-organic vapor phase epitaxy," Phys. Stat. Sol. **211**, 27–33 (2014).
- [44] Tadjer, M. J., Mastro, M. A., Mahadik, N. A., Currie, M., Wheeler, V. D., Freitas, J. A., Greenlee, J. D., Hite, J. K., Hobart, K. D., Eddy, C. R. and Kub, F. J., "Structural, Optical, and Electrical Characterization of Monoclinic β-Ga₂O₃ Grown by MOVPE on Sapphire Substrates," J. Electron. Mater. **45**, 2031–2037 (2016).
- [45] Cora, I., Mezzadri, F., Boschi, F., Bosi, M., Čaplovičová, M., Calestani, G., Dódony, I., Pécz, B. and Fornari, R., "The real structure of ε-Ga ₂ O ₃ and its relation to κ-phase," CrystEngComm **19**(11), 1509–1516 (2017).
- [46] Oshima, Y., Víllora, E. G., Matsushita, Y., Yamamoto, S. and Shimamura, K., "Epitaxial growth of phase-pure ε-Ga₂O₃ by halide vapor phase epitaxy," J. Appl. Phys. **118**(8), 85301 (2015).
- [47] Zhuo, Y., Chen, Z., Tu, W., Ma, X., Pei, Y. and Wang, G., "β-Ga₂O₃ versus ε-Ga₂O₃: Control of the crystal phase composition of gallium oxide thin film prepared by metal-organic chemical vapor deposition," Appl. Surf. Sci. **420**, 802–807 (2017).
- [48] Fornari, R., Pavesi. M., Montedoro, V., Klimm, D., Mezzadri, F., Cora, I., Pécz, B., Boschi, F., Parisini, A., Baraldi, A., Ferrari, C., Gombia, E. and Bosi, M. "Thermal stability of ε-Ga₂O₃ polymorph," Acta Mater. **140**, 411–416 (2017).

- [49] Comstock, D. J. and Elam, J. W., "Atomic Layer Deposition of Ga₂O₃ Films Using Trimethylgallium and Ozone," Chem. Mater. **24**, 4011–4018 (2012).
- [50] Shan, F. K., Liu, G. X., Lee, W. J., Lee, G. H., Kim, I. S. and Shin, B. C., "Structural, electrical, and optical properties of transparent gallium oxide thin films grown by plasmaenhanced atomic layer deposition," J. Appl. Phys. **98**, 23504 (2005).
- [51] Sasaki, K., Kuramata, A., Masui, T., Víllora, E. G., Shimamura, K. and Yamakoshi, S., "Device-Quality β-Ga₂O₃ Epitaxial Films Fabricated by Ozone Molecular Beam Epitaxy," Appl. Phys. Express **5**, 35502 (2012).
- [52] Liu, X. Z., Guo, P., Sheng, T., Qian, L. X., Zhang, W. L. and Li, Y. R., "β-Ga₂O₃ thin films on sapphire pre-seeded by homo-self-templated buffer layer for solar-blind UV photodetector," Opt. Mater. (Amst). **51**, 203–207 (2016).
- [53] Guo, D., Wu, Z., Li, P., An, Y., Liu, H., Guo, X., Yan, H., Wang, G., Sun, C., Li, L. and Tang, W., "Fabrication of β-Ga₂O₃ thin films and solar-blind photodetectors by laser MBE technology," Opt. Mater. Express 4, 1067–1076 (2014).
- [54] Sasaki, K., Higashiwaki, M., Kuramata, A., Masui, T. and Yamakoshi, S., "MBE grown Ga₂O₃ and its power device applications," J. Cryst. Growth **378**, 591–595 (2013).
- [55] Nakagomi, S. and Kokubun, Y., "Crystal orientation of β-Ga₂O₃ thin films formed on c-plane and a-plane sapphire substrate," J. Cryst. Growth **349**, 12–18 (2012).
- [56] Varley, J. B., Weber, J. R., Janotti, A. and Van De Walle, C. G., "Oxygen vacancies and donor impurities in β-Ga₂O₃," Appl. Phys. Lett. **97**, 142106 (2010).
- [57] Wang, G. H., Wong, T. and Wang, X., "Si-Ion Implantation Doping in β-Ga₂O₃ and Its Application to Fabrication of Low-Resistance Ohmic Contacts," Appl. Phys. Express **6**, 86502 (2013).
- [58] Chang, P. C., Fan, Z., Tseng, W. Y., Rajagopal, A. and Lu, J. G., "β-Ga₂O₃ nanowires: Synthesis, characterization, and p-channel field-effect transistor," Appl. Phys. Lett. **87**, 1–3 (2005).
- [59] Liu, L. L., Li, M. K., Yu, D. Q., Zhang, J., Zhang, H., Qian, C. and Yang, Z., "Fabrication and characteristics of N-doped β-Ga₂O₃ nanowires," Appl. Phys. A **98**, 831–835 (2010).
- [60] Chang, L. W., Li, C. F., Hsieh, Y. T., Liu, C. M., Cheng, Y. T., Yeh, J. W. and Shih, H. C., "Ultrahigh-Density β-Ga₂O₃/N-doped β-Ga₂O₃ Schottky and p-n Nanowire Junctions: Synthesis and Electrical Transport Properties," J. Electrochem. Soc. 158(3), D136–D142 (2011).
- [61] Chikoidze, E., Fellous, A., Perez-Tomas, A., Sauthier, G., Tchelidze, T., Ton-That, C., Thanh Huynh, T., Phillips, M., Russell, S., Jennings, M., Berini. B., Jomard, F., Dumont, F. "P-type beta-gallium oxide: A new perspective for power and optoelectronic devices" Materials Today Physics 3 (2017) 118-126
- [62] Lee, C. T. and Yan, J. T., "Sensing mechanisms of Pt/β-Ga₂O₃/GaN hydrogen sensor diodes," Sensors Actuators, B Chem. **147**, 723–729 (2010).
- [63] Ogita, M., Saika, N., Nakanishi, Y. and Hatanaka, Y., "Ga₂O₃ thin films for high-temperature gas sensors," Appl. Surf. Sci. **142**, 188–191 (1999).
- [64] Nakagomi, S., Sai, T. and Kokubun, Y., "Hydrogen gas sensor with self temperature compensation based on β-Ga₂O₃ thin film," Sensors Actuators, B Chem. **187**, 413–419 (2013).

- [65] Pohle, R., Weisbrod, E. and Hedler, H., "ScienceDirect Enhancement of MEMS-based Ga₂O₃ gas sensors by surface modifications," Procedia Eng. **168**, 211–215 (2016).
- [66] Chang, S.-J., Wu, Y.-L., Weng, W.-Y., Lin, Y.-H., Hsieh, W.-K., Sheu, J.-K. and Hsu, C.-L., "Ga₂O₃ Films for Photoelectrochemical Hydrogen Generation," J. Electrochem. Soc. **161**, H508–H511 (2014).
- [67] Takayoshi, O., Kaminaga, K., Mashiko, H., Mukai, A., Sasaki, K., Masui, T., Kuramata, A., Yamakoshi, S. and Ohtomo, A., "β-Ga₂O₃ Single Crystal as a Photoelectrode for Water Splitting," Jpn. J. Appl. Phys. **52**, 111102 (2013).
- [68] Razeghi, M. and Rogalski, A., "Semiconductor ultraviolet detectors," J. Appl. Phys. **79**(10), 7433–7473 (1996).
- [69] Chen, H., Liu, K., Hu, L., Al-Ghamdi, A. A. and Fang, X., "New concept ultraviolet photodetectors," Mater. Today **18**(9), 493–502 (2015).
- [70] Alaie, Z., Nejad, S. M. and Yousefi, M. H., "Recent advances in ultraviolet photodetectors," Mater. Sci. Semicond. Process. **29**, 16–55 (2015).
- [71] Zhang, W., Xu, J., Ye, W., Li, Y., Qi, Z., Dai, J., Wu, Z., Chen, C., Yin, J., Li, J., Jiang, H. and Fang, Y., "High-performance AlGaN metal-semiconductor-metal solar-blind ultraviolet photodetectors by localized surface plasmon enhancement," Appl. Phys. Lett. **106**, 21112 (2015).
- [72] Hou, Y., Mei, Z. and Du, X., "Semiconductor ultraviolet photodetectors based on ZnO and MgxZn1-xO," J. Phys. D. Appl. Phys. 47, 283001 (2014).
- [73] Huang, L., Feng, Q., Han, G., Li, F., Li, X., Fang, L., Xing, X., Zhang, J. and Hao, Y., "Comparison Study of β-Ga₂O₃ Photodetectors Grown on Sapphire at Different Oxygen Pressures," IEEE Photonics J. **9**(4), 6803708 (2017).
- [74] Zhao, X., Cui, W., Wu, Z., Guo, D., Li, P., An, Y., Li, L. and Tang, W., "Growth and Characterization of Sn Doped β-Ga₂O₃ Thin Films and Enhanced Performance in a Solar-Blind Photodetector," J. Electron. Mater. **46**, 2366–2372 (2017).
- [75] Singh Pratiyush, A., Krishnamoorthy, S., Vishnu Solanke, S., Xia, Z., Muralidharan, R., Rajan, S. and Nath, D. N., "High responsivity in molecular beam epitaxy grown β-Ga₂O₃ metal semiconductor metal solar blind deep-UV photodetector," Appl. Phys. Lett. **110**, 221107 (2017).
- [76] Zhang, F., Li, H., Arita, M. and Guo, Q., "Ultraviolet detectors based on (GaIn)₂O₃ films," Opt. Mater. Express 7(10), 3769 (2017).
- [77] Alema, F., Hertog, B., Ledyaev, O., Volovik, D., Thoma, G., Miller, R., Osinsky, A., Mukhopadhyay, P., Bakhshi, S., Ali, H. and Schoenfeld, W. V., "Solar blind photodetector based on epitaxial zinc doped Ga₂O₃ thin film," Phys. Status Solidi Appl. Mater. Sci. **214**, 1600688 (2017).
- [78] Wu, Z., Bai, G., Qu, Y., Guo, D., Li, L., Li, P., Hao, J. and Tang, W., "Deep ultraviolet photoconductive and near-infrared luminescence properties of Er3+-doped β-Ga₂O₃ thin films," Appl. Phys. Lett. **108**(21), 1–5 (2016).
- [79] Oshima, T., Okuno, T. and Fujita, S., "Ga₂O₃ thin film growth on c-plane sapphire substrates by molecular beam epitaxy for deep-ultraviolet photodetectors," Jpn. J. Appl. Phys. **46**, 7217–7220 (2007).
- [80] Wuu, D.-S., Ou, S.-L., Horng, R.-H., Ravadgar, P., Wang, T.-Y. and Lee, H.-Y., "Growth and characterization of Ga₂O₃ on sapphire substrates for UV sensor applications," Proc. SPIE **8263**, 826317 (2012).

- [81] Othonos, K. M., Zervos, M., Christofides, C. and Othonos, A., "Ultrafast Spectroscopy and Red Emission from β-Ga₂O₃/β-Ga₂S₃ Nanowires," Nanoscale Res. Lett. **10**(1), 304 (2015).
- [82] Othonos, A., Zervos, M. and Christofides, C., "Carrier dynamics in β-Ga₂O₃ nanowires," J. Appl. Phys. **108**(12), 124302 (2010).
- [83] Yasukawa, D., Wakai, H., Oda, H. and Yamanaka, A., "Effect of Transition Metals on Optical Properties of β-Ga₂O₃: Time-Resolved Spectroscopy," IOP Conf. Ser. Mater. Sci. Eng. **18**(10), 102023 (2011).
- [84] Oh, S., Jung, Y., Mastro, M. A., Hite, J. K., Eddy, C. R. and Kim, J., "Development of solar-blind photodetectors based on Si-implanted β-Ga₂O₃," Opt. Express **23**(22), 28300 (2015).
- [85] Guo, D. Y., Shi, H. Z., Qian, Y. P., Lv, M., Li, P. G., Su, Y. L., Liu, Q., Chen, K., Wang, S. L., Cui, C., Li, C. R. and Tang, W. H., "Fabrication of β-Ga₂O₃/ZnO heterojunction for solar-blind deep ultraviolet photodetection," Semicond. Sci. Technol. 32(3), 03LT01 (2017).
- [86] Photodetector, A. O. G. S., Weng, W. Y., Hsueh, T. J., Chang, S. J., Member, S., Huang, G. J. and Hsueh, H. T., "A β-Ga₂O₃/GaN Schottky-Barrier Photodetector," IEEE PHOTONICS Technol. Lett. **23**(7), 444–446 (2011).
- [87] Matsuzaki, K., Hiramatsu, H., Nomura, K., Yanagi, H., Kamiya, T., Hirano, M. and Hosono, H., "Growth, structure and carrier transport properties of Ga₂O₃ epitaxial film examined for transparent field-effect transistor," Thin Solid Films **496**(1), 37–41 (2006).
- [88] Tomm, Y., Ko, J. M., Yoshikawa, A. and Fukuda, T., "Floating zone growth of β-Ga₂O₃: A new window material for optoelectronic device applications," Sol. Energy Mater. Sol. Cells **66**(1–4), 369–374 (2001).
- [89] Víllora, E. G., Arjoca, S., Shimamura, K., Inomata, D. and Aoki, K., "β-Ga₂O₃ and single-crystal phosphors for high-brightness white LEDs and LDs, and β-Ga₂O₃ potential for next generation of power devices," Proc. SPIE(March 2014), 89871U (2014).
- [90] Villora, E. G., Shimamura, K., Yoshikawa, Y., Aoki, K. and Ichinose, N., "Large-size β-Ga₂O₃ single crystals and wafers," J. Cryst. Growth **270**(3–4), 420–426 (2004).
- [91] Zhang, J., Li, B., Xia, C., Pei, G., Deng, Q., Yang, Z., Xu, W., Shi, H., Wu, F., Wu, Y. and Xu, J., "Growth and spectral characterization of β-Ga₂O₃ single crystals," J. Phys. Chem. Solids **67**(12), 2448–2451 (2006).
- [92] Suzuki, N., Ohira, S., Tanaka, M., Sugawara, T., Nakajima, K. and Shishido, T., "Fabrication and characterization of transparent conductive Sn-doped β-Ga₂O₃ single crystal," Phys. Status Solidi Curr. Top. Solid State Phys. 4(7), 2310–2313 (2007).
- [93] Aida, H., Nishiguchi, K., Takeda, H., Aota, N., Sunakawa, K. and Yaguchi, Y., "Growth of β-Ga₂O₃ single crystals by the edge-defined, film fed growth method," Jpn. J. Appl. Phys. 47(11), 8506–8509 (2008).
- [94] Galazka, Z., Uecker, R., Irmscher, K., Albrecht, M., Klimm, D., Pietsch, M., Brützam, M., Bertram, R., Ganschow, S. and Fornari, R., "Czochralski growth and characterization of β-Ga₂O₃ single crystals," Cryst. Res. Technol. **45**(12), 1229–1236 (2010).
- [95] Galazka, Z., Irmscher, K., Uecker, R., Bertram, R., Pietsch, M., Kwasniewski, A., Naumann, M., Schulz, T., Schewski, R., Klimm, D. and Bickermann, M., "On the bulk β-Ga₂O₃ single crystals grown by the Czochralski method," J. Cryst. Growth **404**, 184–191 (2014).
- [96] Higashiwaki, M., Sasaki, K., Kuramata, A., Masui, T. and Yamakoshi, S., "Development of gallium oxide power devices," Phys. Status Solidi Appl. Mater. Sci. **211**, 21–26 (2014).
- [97] Higashiwaki, M., Sasaki, K., Kamimura, T., Hoi Wong, M., Krishnamurthy, D., Kuramata, A., Masui, T. and Yamakoshi, S., "Depletion-mode Ga₂O₃ metal-oxide-semiconductor field-

- effect transistors on β-Ga₂O₃ (010) substrates and temperature dependence of their device characteristics," Appl. Phys. Lett. **103**, 1–5 (2013).
- [98] Kim, J., Oh, S., Mastro, M. A. and Kim, J., "Exfoliated β-Ga₂O₃ nano-belt field-effect transistors for air-stable high power and high temperature electronics," Phys. Chem. Chem. Phys. **18**(23), 15760–15764 (2016).